



Mercury isotopes in frozen soils reveal transboundary atmospheric mercury deposition over the Himalayas and Tibetan Plateau[☆]

Jie Huang^{a, c, *}, Shichang Kang^{b, c, g}, Runsheng Yin^d, Junming Guo^b, Ryan Lepak^e, Sillanpää Mika^f, Lekhendra Tripathee^b, Shiwei Sun^{b, g}

^a Key Laboratory of Tibetan Environment Changes and Land Surface Processes, Institute of Tibetan Plateau Research, Chinese Academy of Sciences, Beijing, 100101, China

^b State Key Laboratory of Cryospheric Science, Northwest Institute of Eco-Environment and Resources, Chinese Academy of Sciences, Lanzhou, 730000, China

^c CAS Center for Excellence in Tibetan Plateau Earth Sciences, Chinese Academy of Sciences, Beijing, 100101, China

^d State Key Laboratory of Ore Deposit Geochemistry, Institute of Geochemistry, Chinese Academy of Sciences, Guiyang, 550002, China

^e Environmental Chemistry and Technology Program, University of Wisconsin-Madison, Madison, WI, 53706, USA

^f Laboratory of Green Chemistry, School of Engineering Science, Lappeenranta University of Technology, Mikkeli, FI-50130, Finland

^g University of the Chinese Academy of Sciences, Beijing, 100049, China

ARTICLE INFO

Article history:

Received 8 July 2019

Received in revised form

12 October 2019

Accepted 17 October 2019

Available online 18 October 2019

Keywords:

Mercury

Transboundary pollution

Frozen soil

Himalaya-Tibet

ABSTRACT

The concentration and isotopic composition of mercury (Hg) were studied in frozen soils along a southwest-northeast transect over the Himalaya-Tibet. Soil total Hg (Hg_T) concentrations were significantly higher in the southern slopes ($72 \pm 54 \text{ ng g}^{-1}$, 2SD, $n = 21$) than those in the northern slopes ($43 \pm 26 \text{ ng g}^{-1}$, 2SD, $n = 10$) of Himalaya-Tibet. No significant relationship was observed between Hg_T concentrations and soil organic carbon (SOC), indicating that the Hg_T variation was not governed by SOC. Soil from the southern slopes showed significantly negative mean $\delta^{202}\text{Hg}$ ($-0.53 \pm 0.50\%$, 2SD, $n = 21$) relative to those from the northern slopes ($-0.12 \pm 0.40\%$, 2SD, $n = 10$). The $\delta^{202}\text{Hg}$ values of the southern slopes are more similar to South Asian anthropogenic Hg emissions. A significant correlation between $1/Hg_T$ and $\delta^{202}\text{Hg}$ was observed in all the soil samples, further suggesting a mixing of Hg from South Asian anthropogenic emissions and natural geochemical background. Large ranges of $\Delta^{199}\text{Hg}$ (-0.45 and 0.24%) were observed in frozen soils. Most of soil samples displayed negative $\Delta^{199}\text{Hg}$ values, implying they mainly received Hg from gaseous $Hg(0)$ deposition. A few samples had slightly positive odd-MIF, indicating precipitation-sourced Hg was more prevalent than gaseous $Hg(0)$ in certain areas. The spatial distribution patterns of Hg_T concentrations and Hg isotopes indicated that Himalaya-Tibet, even its northern part, may have been influenced by transboundary atmospheric Hg pollution from South Asia.

© 2019 Elsevier Ltd. All rights reserved.

1. Introduction

Known as the “Third Pole”, the Himalayas and Tibetan Plateau region (hereinafter Himalaya-Tibet) is one of the most impressive topographic features on the surface of the Earth with an average altitude of over 4000 m above sea level (a.s.l.) (Qiu, 2008).

Himalaya-Tibet mainly consists of high mountains, glaciers, and frozen ground. In particular, the frozen ground bodies on Himalaya-Tibet (Fig. S1) constitutes the largest permafrost region in the low- and mid-latitudes, which accounts for 74.5% of the Northern Hemisphere's high-mountain permafrost (Jin et al., 2000).

Due to its remote location, unique landform and isolated ecosystems, Himalaya-Tibet is sensitive to anthropogenic impacts (Yao et al., 2012). Since middle and eastern China are located in downwind of the Westerlies (Fig. 1), anthropogenic emissions from these areas are believed to have a limited impact to Himalaya-Tibet. The large-scale atmospheric circulation patterns over Himalaya-Tibet is dominantly governed by the South Asian monsoon, that carries massive atmospheric contamination from South Asia to the region

[☆] This paper has been recommended for acceptance by Prof. Wen-Xiong Wang.

* Corresponding author. Key Laboratory of Tibetan Environment Changes and Land Surface Processes, Institute of Tibetan Plateau Research, Chinese Academy of Sciences, Beijing, 100101, China.

E-mail address: huangjie@itpcas.ac.cn (J. Huang).

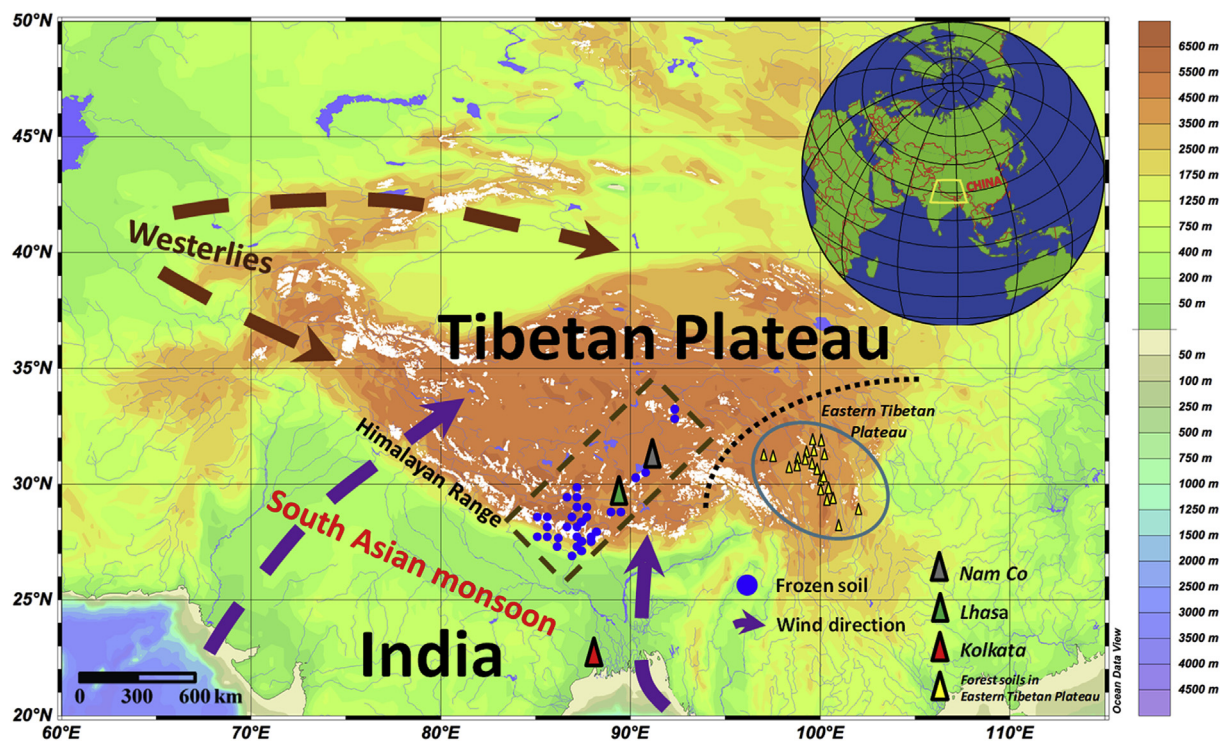


Fig. 1. Map showing the locations of sampling sites of frozen soils in Himalaya-Tibet. (This figure was generated by Ocean Data View, Latest ODV4 Version: ODV 4.7.10, which is available at <http://odv.awi.de/>).

(Sheng et al., 2013; Lüthi et al., 2015; Huang et al., 2016). Due to the rapid economic development in the past decades, South Asia has become one of the world's largest sources of anthropogenic contaminants emitted into the atmosphere (Mukherjee et al., 2009; Burger Chakraborty et al., 2013). As such, the South Asian monsoon is an important transporter of enhanced air pollution into the inland Tibetan Plateau, as supported by evidence of increased pollution from atmospheric contaminants such as black carbon (Cong et al., 2013), Persistent Organic Pollutants (POPs) (Yang et al., 2016) and mercury (Hg) (Yang et al., 2010; Huang et al., 2015; Kang et al., 2016) have been observed over the last decades.

Of particular interest among the air pollutants is Hg (UNEP, 2013), a globally distributed semi-volatile pollutant. Similar to alpine regions (Obrist et al., 2017; Schuster et al., 2018), there is growing evidence that mountain regions of the Tibetan Plateau could act as a sink of atmospheric Hg (Huang et al., 2012; Wang et al., 2017). In remote areas such as Himalaya-Tibet, frozen soils primarily receive Hg from the atmosphere through wet deposition (e.g., precipitation, snow) and dry deposition (e.g., litterfall, direct uptake of gaseous elemental Hg (Hg(0) or GEM), gaseous oxidized Hg (GOM) and particulate bound Hg (PBM)), due to the lack of direct anthropogenic Hg emission sources. Although Hg concentrations in soils have been widely used to document atmospheric Hg deposition (Tipping et al., 2011; Sheng et al., 2012; Liu et al., 2016), Hg concentrations can hardly distinguish the sources and geochemical fate of Hg.

Hg isotope geochemistry has become a useful tracer to discriminate sources and pathways of Hg in the environment. Hg isotopes not only undergo mass-dependent fractionation (MDF, denoted as $\delta^{202}\text{Hg}$), but also mass-independent fractionation (MIF, denoted as $\Delta^{199}\text{Hg}$ and $\Delta^{200}\text{Hg}$) during complicated biogeochemical Hg cycling (Blum et al., 2014). MDF occurs during various biogeochemical processes, while MIF only occurs during a few processes such as photochemical reactions and equilibrium Hg²⁺-

thiol complexation (Blum et al., 2014). The observed odd-MIF in natural samples is primarily the result of aqueous Hg(II) photoreduction and photochemical demethylation (Bergquist and Blum, 2007), whereas even-MIF in natural samples is likely caused by atmospheric Hg(0) photo-oxidation (Gratz et al., 2010; Chen et al., 2012; Demers et al., 2013; Sun et al., 2016). Large variations in $\delta^{202}\text{Hg}$ and $\Delta^{199}\text{Hg}$ ($\sim 10\%$ for both), and $\Delta^{200}\text{Hg}$ ($\sim 1\%$) have been reported for different Hg pools (Blum et al., 2014). With knowledge of the Hg isotopic signatures of known sources and isotope fractionation processes, Hg isotope mixing models can be used to evaluate the contribution of Hg from different sources to soils (Zhang et al., 2013).

To our best knowledge, there are currently few measurements of Hg isotopic compositions from Himalaya-Tibet existing in literature on the systematics of Hg stable isotopes. A recent study reported negative $\delta^{202}\text{Hg}$ (-2.98 to -0.69%) and $\Delta^{199}\text{Hg}$ (-0.46 to -0.04%) values in surface frozen soils from the forests (hereafter, forest soil) of the eastern Tibetan Plateau, concluded that Hg(0) uptake in foliage, followed by litterfall was the major pathway of Hg accumulation in soils (Wang et al., 2017). Compared with the eastern Tibetan Plateau is dominated by montane forested areas (e.g., trees, shrubs) (Fig. S1), however, the Himalaya-Tibet is located in more closer to South Asia (Fig. 1) and is mainly covered by lichen or short grasses in the frozen soil, which is similar to the Arctic (Olson et al., 2019). Due to different geographies and landscapes, we hypothesize that the Hg sources and deposition pathways in our study region may be different from the eastern Tibetan Plateau. Moreover, a recent study reported negative $\delta^{202}\text{Hg}$ (-1.33 to -0.77%) and $\Delta^{199}\text{Hg}$ values (-0.33 to 0%) in tundra vegetation/soils in the Arctic (Obrist et al., 2017), highlighting the fact that frozen ground mainly receives Hg from direct atmospheric Hg(0) deposition. Therefore, a similar case may also occur in the frozen soils of Himalaya-Tibet.

In this work, we conducted a comprehensive study on frozen soils sampled along a southwest-northeast transect over Himalaya-

Tibet. The spatial variations of Hg concentrations and isotopic compositions of frozen soils were quantified. We aimed (1) to test whether anthropogenic Hg emissions from South Asia could have a direct impact to Himalaya-Tibet; (2) to understand the pathways of atmospheric Hg deposition (wet versus dry deposition) on Himalaya-Tibet.

2. Materials and methods

2.1. Study area and sample collection

From March to April of 2013, a total of 31 surface frozen soil samples (~5 cm) were collected from the frozen ground (>3000 m a.s.l) along a southwest-northeast transect over Himalaya-Tibet (Fig. 1). Among them, 21 samples were collected from the southern slopes of the Himalayas (i.e., Nepal Himalaya), and 10 from the northern slopes (Table S1). The mean annual temperature and precipitation of the study area decrease from southwest to northeast, varying approximately from 3 °C to -2.9 °C (Xu et al., 2006) and from 700 mm yr⁻¹ to 50 mm yr⁻¹ (Kang et al., 2010), respectively.

All samples were collected into high density polyethylene (HDPE) plastic bags and stored a cooler box (4 °C). The samples were then freeze-dried at -70 °C for 120 h until evaporation was no longer observed (until a mass variation of <0.05% in the next 8 h). After that, soil samples were ground by agate mortar to 200 mesh sieve (74 μm), and stored in new polyethylene plastic bags. Alcohol was used to wash the mortar after each sample grinding to prevent cross contamination.

2.2. Total Hg and soil organic carbon analysis

Total Hg (Hg_T) concentrations of the samples were measured by the Leeman Hydra-IIC direct Hg analyzer (Leeman Lab Hydra, Hudson, NH), following the US EPA method 7473. The method detection limit (MDL) for soil samples, defined as 3 times the standard deviation of 10 replicates measurements of sample blanks, was less than 0.1 ng g⁻¹ and the relative standard deviations (RSDs) for the replicate samples were less than 5%. The standard reference material (32 ng g⁻¹, lake sediment GSS-9) was interspersed with every 5 samples for external quality control, which yielded the recoveries of 98 ± 6% (n = 6).

The measurements of soil organic carbon content (SOC, in %) were conducted on a PerkinElmer 2400 Series II CHNSO Elemental Analyzer (United Kingdom, limit of detection ≤ 10 ppm) by a combustion methods. The frozen soil samples were first rinsed with 10% (v/v) aqueous HCl solution for 24 h to remove inorganic carbon present in the form of carbonates. The carbonate-free samples were then dried at 40 °C for 48 h. The SOC content was measured by determining the percent loss of weight on ignition. Duplicated measurements for SOC were performed, and the accepted change of replicated measurements was <5%. Standard reference materials IVA99994 were measured in every 5 samples that yielded recoveries of 95–105%. More details about the analytical methods for Hg_T and SOC can be found elsewhere (Huang et al., 2019).

2.3. Hg isotopic composition analysis

About 0.4–0.5 g of soil samples and certified reference materials (MESS-2) were digested (95 °C, 12 h) using 5 mL aqua regia (HCl: HNO₃ = 3:1, v/v). The digests were diluted to 0.5 ng mL⁻¹ Hg and 10–20% acids, based on the measured Hg concentrations (Table S1), prior to isotopic measurement at the Wisconsin State Laboratory of Hygiene, using the Neptune Plus multi-collector inductively

coupled plasma mass spectrometry (Yin et al., 2016a). Hg concentrations and acid matrices of the NIST SRM 3133 Hg standard were matched to the bracketed samples. δ²⁰²Hg, Δ¹⁹⁹Hg, and Δ²⁰¹Hg were calculated relative to NIST SRM 3133 Hg standard solution, following recommended nomenclature (Bergquist and Blum, 2007).

UM-Almadén secondary standard solutions with similar Hg concentrations and acid matrices were measured. Our results about UM-Almadén: (δ²⁰²Hg: -0.51 ± 0.08‰; Δ¹⁹⁹Hg: -0.03 ± 0.04‰; Δ²⁰⁰Hg: 0.02 ± 0.04‰, 2SD, n = 3) and MESS-2 (δ²⁰²Hg: -1.95 ± 0.03‰; Δ¹⁹⁹Hg: 0.01 ± 0.04‰; Δ²⁰⁰Hg: 0.05 ± 0.04‰, 2SD, n = 3) were consistent with the reported values (Lepak et al., 2015; Xu et al., 2016; Yin et al., 2016b).

3. Results and discussion

3.1. Hg concentrations in frozen soils

Hg_T concentrations from all of the frozen soils varied from 24 to 255 ng g⁻¹, with a mean of 63 ± 47 ng g⁻¹ (2SD, n = 31) (Table S1) that is higher than the average concentration of Hg in topsoils from the Tibetan Plateau (mean = 37 ng g⁻¹, Sheng et al. (2012)). The mean frozen soil Hg concentration in the southern slopes (72 ± 54 ng g⁻¹, 2SD, n = 21) is statistically about twice as high as the northern slopes (43 ± 26 ng g⁻¹, 2SD, n = 10) (p < 0.05, T-test). Although soil organic matter is known to bind strongly with Hg (Ravichandran, 2004) and is a well-documented factor that controls the Hg concentrations in soils (Sheng et al., 2012; Sun et al., 2017), frozen soils from both slopes showed similar SOC values, 1.69 ± 0.78% and 1.77 ± 0.95% for the southern and northern slopes (Table S1), respectively. No clear correlation was found between Hg_T and SOC for our samples from the northern or southern slopes (Fig. S2), indicating that SOC is not the major driver for the spatial variations of Hg_T. Numerous studies have suggested that the atmospheric contaminants deposition over Himalaya-Tibet has been greatly altered by anthropogenic perturbations from South Asia (Cong et al., 2013; Sheng et al., 2013; Lüthi et al., 2015; Yang et al., 2016). Considering its close proximity and the influence of South Asia monsoon circulation, previous studies hypothesized that anthropogenic Hg emitted from South Asia could be long-range transported to Himalaya-Tibet (Yang et al., 2010; Huang et al., 2015; Kang et al., 2016). The decrease of average Hg_T concentration from the southern to northern slopes indicates South Asia may be an important source region of Hg to Himalaya-Tibet.

3.2. Mass-dependent fractionation

δ²⁰²Hg values of all frozen soils vary from -1.43 to 0.69‰ with an average of -0.40 ± 0.50‰ (2SD, n = 31) (Table S1), within the ranges previously reported for soil samples from different sites of the world (-5.0 to 1.0‰, Blum et al. (2014)). Compared to the forest soils from the eastern Tibetan Plateau (δ²⁰²Hg: -2.98 to -0.69‰, Wang et al. (2017)), as shown in Fig. 2, our samples showed significantly higher δ²⁰²Hg values (p < 0.01, T-test). Previous studies suggested that background soils at forest areas are largely altered by the negative MDF (-3 to -1‰) during adsorption of Hg(0) by foliage (Demers et al., 2013; Zheng et al., 2016). Therefore, the more negative δ²⁰²Hg in forest soils from the eastern Tibetan Plateau can be greatly attributed to the inputs of litterfall which favors adsorption of isotopically light Hg(0) by foliage as reported in many previous studies (Demers et al., 2013; Zheng et al., 2016). The relatively higher δ²⁰²Hg values of our samples may be explained by the different vegetation cover in Himalaya-Tibet (Fig. S1). As mentioned earlier, the ground vegetation cover in our study area

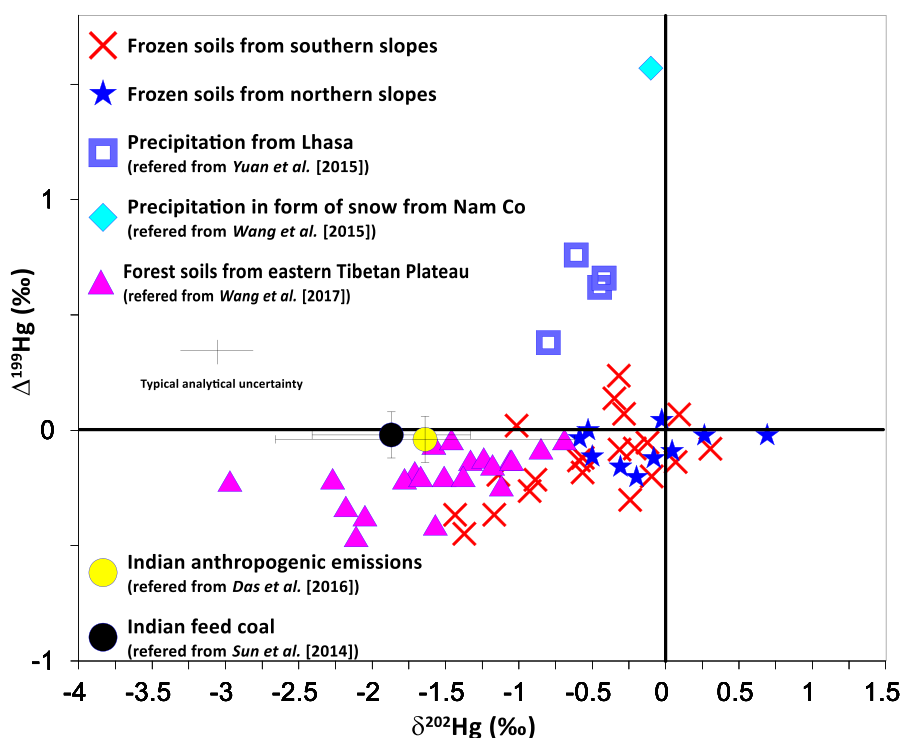


Fig. 2. $\Delta^{199}\text{Hg}$ vs $\delta^{202}\text{Hg}$ for frozen soils from Himalaya-Tibet, forest soils from eastern Tibetan Plateau, precipitation from Lhasa, snow from Nam Co, Tibet, and anthropogenic emissions from India. The sampling locations of eastern Tibetan Plateau (Wang et al., 2017), Nam Co (Yuan et al., 2015), Lhasa (Wang et al., 2015) and Kolkata (Das et al., 2016) are illustrated in Fig. 1.

mainly includes moss, lichen and grasses, which have markedly lower biomass densities than those in forest areas. Low biomass density causes less adsorption of isotopically light Hg by vegetation cover in the frozen soils (Fig. 2). Due to the Arctic frozen ground is also absent of forest cover, tundra soils also showed relatively higher $\delta^{202}\text{Hg}$ values (-0.77 to -1.33‰ , Obrist et al. (2017)).

Frozen soils from the southern slopes showed significantly negative $\delta^{202}\text{Hg}$ (-1.43 to 0.31‰ , mean = $-0.53 \pm 0.50\text{‰}$, 2SD, $n=21$) values compared to those from the northern slopes (-0.59 – 0.69‰ , mean = $-0.12 \pm 0.40\text{‰}$, 2SD, $n=10$) ($p < 0.05$, T-test) (Table S1). Variations in vegetation is an unlikely driver for the $\delta^{202}\text{Hg}$ differences between the two slopes since significant correlations between Hg_T and SOC were not observed (Fig. S2). The isotopic compositions of Hg in soils have been widely used to reveal the changes of Hg sources (Feng et al., 2010; Zhang et al., 2013). Similarly, the isotopic variations in frozen soils more likely reflect the changes of Hg sources in our study. The isotopic signatures of Indian anthropogenic Hg sources (e.g., industrial and traffic emissions, and waste incineration) (Das et al., 2016) and Indian feed coal (Sun et al., 2014) in South Asia showed an average $\delta^{202}\text{Hg}$ value of $-1.64 \pm 1.02\text{‰}$ (2SD, $n=52$) and $-1.87 \pm 0.54\text{‰}$ (2SD, $n=12$) (Fig. 2), respectively. According to Sun et al. (2014), Hg isotopic signatures of coal combustion emissions are likely shifted to more negative $\delta^{202}\text{Hg}$ values for PBM (by -0.50‰) and more positive $\delta^{202}\text{Hg}$ values for GOM (by $+0.1\text{‰}$) and GEM (by $+1.1\text{‰}$) relative to feed coal. When we take Hg speciation into account, the $\delta^{202}\text{Hg}$ values in Indian coal combustion were grossly estimated to range from -2.37‰ (PBM) to -0.77‰ (GEM). As shown in Fig. 3, the $\delta^{202}\text{Hg}$ values of frozen soils from southern slopes are more similar to that of the anthropogenic Hg emissions from South Asia. A linear correlation between $\delta^{202}\text{Hg}$ and $1/\text{Hg}_T$ was observed for our soil samples (Fig. 3), indicating the mixing of two Hg sources. It is noteworthy that anthropogenic Hg sources from South Asia fit well

as an end member for this correlation line (Fig. 3). We predict the other end-member, that reflects the geochemical background, would be characterized by much lower Hg concentrations and higher $\delta^{202}\text{Hg}$ values (-0.5 – 1‰). The term of “geochemical background” is defined as soil that contains Hg mainly originated from natural (or geogenic) sources (Kicińska and Turek, 2017). This is supported by the three points on the far right (Fig. 3), which demonstrated the lowest Hg_T concentration and high $\delta^{202}\text{Hg}$ values, were collected from the further north high-elevation sites (Table S1). The Himalaya-Tibet mainly exposes a spectacular assemblage of metamorphic rocks which were formed during the Himalayan continental collisions (Kohn, 2014). According to Xu et al. (2018), metamorphic rocks from the Tibetan Plateau have been shown low Hg_T (10 – 150 ng g^{-1}) and high $\delta^{202}\text{Hg}$ values (-0.98 to 0.62‰). While $\delta^{202}\text{Hg}$ -based binary mixing models have been used by many previous studies to estimate the amount of Hg from anthropogenic and natural background sources in soils (Zhang et al., 2013) and sediments (Foucher et al., 2009), we will not go further in our study at this time considering the complexity of isotope fractionation during long-range transport and post-emission processes, and the uncertainty of Hg isotope signatures from the two Hg sources in such a large study area.

3.3. Mass-independent fractionation

$\Delta^{199}\text{Hg}$ values of all frozen soils fluctuate between -0.45 and 0.24‰ with an average of $-0.11 \pm 0.15\text{‰}$ (2SD, $n=31$) (Table S1). The $\Delta^{199}\text{Hg}$ values range from -0.45 to 0.24‰ , and from -0.20 to 0.04‰ , for soils in the southern and northern slopes, respectively (Fig. 2 and Table S1). Two potential pathways have been understood to cause the MIF of ^{199}Hg and ^{201}Hg in soils: Hg(II) photoreduction and Hg(II) dark reduction, in the presence of natural organic matter (Bergquist and Blum, 2007; Zheng and Hintelmann, 2009; Jiskra

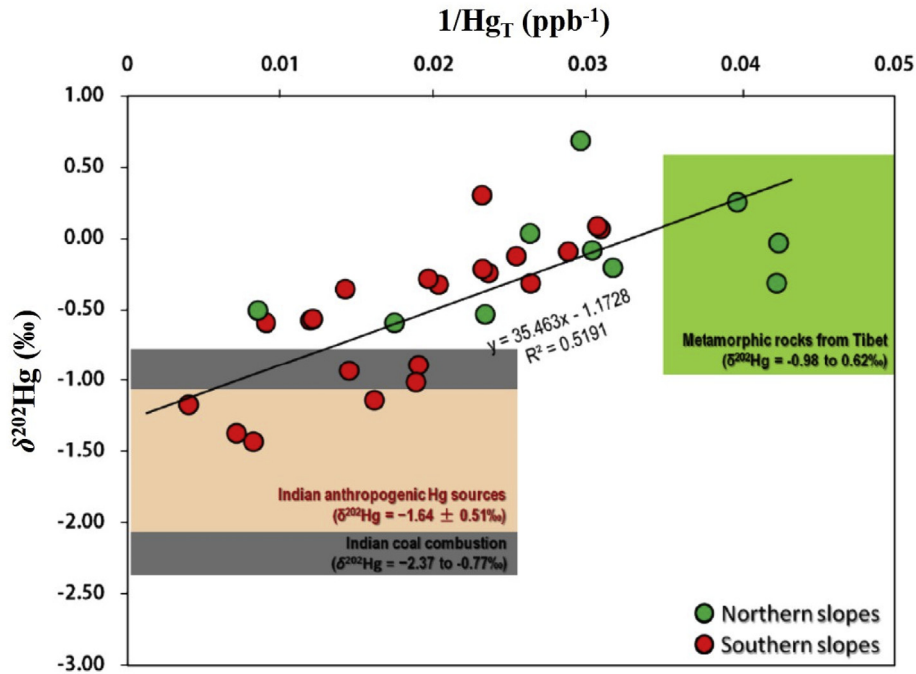


Fig. 3. $\delta^{202}\text{Hg}$ (‰) versus $1/\text{Hg}_T$ (ppb^{-1}) for frozen soils in Himalaya-Tibet indicates a binary mixing of anthropogenic Hg and geochemical background. $\delta^{202}\text{Hg}$ values in anthropogenic end members were referred from [Das et al. \(2016\)](#) and [Sun et al. \(2014\)](#), and geochemical background end members from [Xu et al. \(2018\)](#), respectively.

[et al., 2015](#)). Hg(II) photoreduction is associated with $\Delta^{199}\text{Hg}/\Delta^{201}\text{Hg}$ of about 1 ([Bergquist and Blum, 2007](#)), whereas Hg(II) dark reduction is associated with $\Delta^{199}\text{Hg}:\Delta^{201}\text{Hg}$ of about 1.6 ([Jiskra et al., 2015](#)). The slope of about 0.92 for $\Delta^{199}\text{Hg}/\Delta^{201}\text{Hg}$ was

obtained in our study ([Fig. 4](#)), consistent with that observed during aqueous Hg(II) photo-reduction ([Bergquist and Blum, 2007](#)), suggesting that Hg has undergone aqueous Hg(II) photo-reduction before being incorporated into our samples. A recent study in a

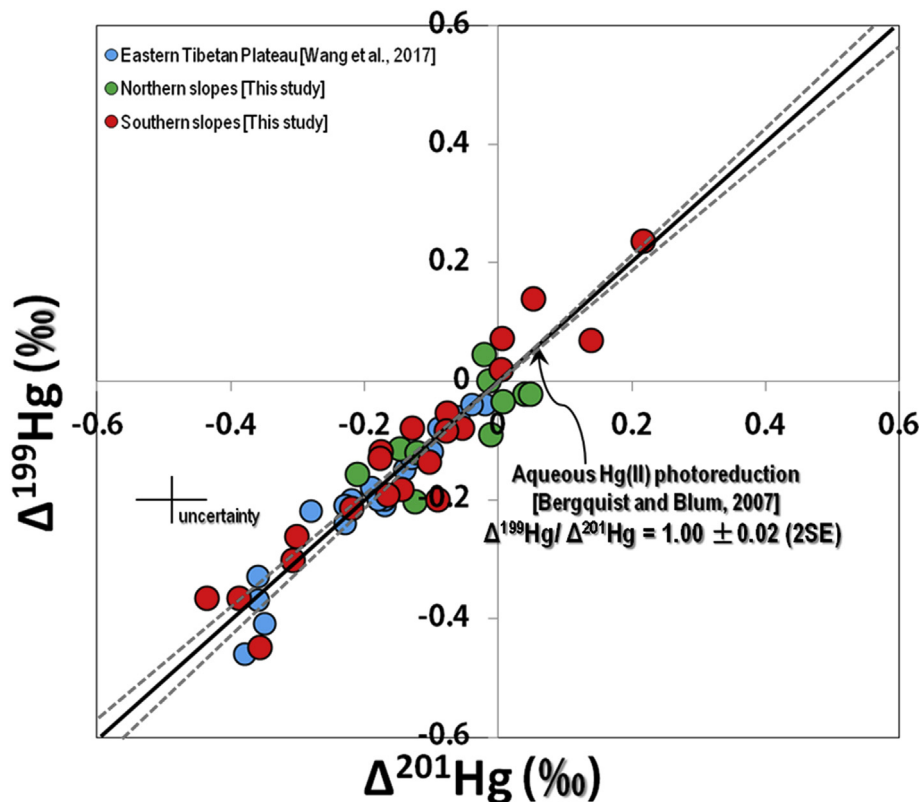


Fig. 4. $\Delta^{199}\text{Hg}$ vs $\Delta^{201}\text{Hg}$ for frozen soils and forest soils in Himalaya-Tibet.

coniferous forest of Sweden demonstrated that Hg(II) dark reduction can occur in histosols (peat soils) and result in a higher $\Delta^{199}\text{Hg}/\Delta^{201}\text{Hg}$ ~1.25 (Jiskra et al., 2015). However, this effect seems to be limited in our frozen soil samples, probably due to the low SOC level of frozen soil or different degree of soil saturation compared to the much higher SOC in peat soils (Jiskra et al., 2015).

The MIF of ^{199}Hg and ^{201}Hg have been used to discriminate between the deposition pathways of atmospheric Hg (e.g. (Demers et al., 2013; Jiskra et al., 2015)). Negative $\Delta^{199}\text{Hg}$ values have been observed in gaseous Hg(0) and positive $\Delta^{199}\text{Hg}$ values were observed in oxidized Hg(II) species in the atmosphere (Rolison et al., 2013). Atmospheric Hg enters the soils mainly through precipitation and litterfall, and these two pathways exhibit distinct MIF patterns. While not completely understood mechanistically, plant materials appear to favor Hg(0) absorption and therefore exhibit negative $\Delta^{199}\text{Hg}$ values (Demers et al., 2013; Yin et al., 2013; Jiskra et al., 2015; Zheng et al., 2016). Atmospheric Hg(II) species are more easily scavenged by precipitation due to their high solubility, therefore precipitation, including those collected from the Tibetan Plateau (Fig. 2), are characterized by positive $\Delta^{199}\text{Hg}$ values (Gratz et al., 2010; Chen et al., 2012; Sherman et al., 2012; Wang et al., 2015; Yuan et al., 2015).

In our study, most samples showed slightly negative $\Delta^{199}\text{Hg}$ values, despite a few samples from the southern slopes which showed slightly positive $\Delta^{199}\text{Hg}$ values (Figs. 2 and 4). The slightly negative MIF in frozen soils is consistent with that previously observed in vegetation (Demers et al., 2013; Wang et al., 2017), peat (Enrico et al., 2016), and tundra vegetation/soils in the Arctic (Obrist et al., 2017) as a result of Hg(0) uptake. While Himalaya-Tibet is predominantly covered by frozen ground rather than forest area, we suggest that the retention of atmospheric Hg(0) by frozen soils or direct uptake of Hg(0) followed by oxidation are the major pathways of atmospheric Hg deposition to the frozen ground. The few frozen soil samples with positive $\Delta^{199}\text{Hg}$ values were mostly collected from the southern slopes (Fig. 2), suggesting the scavenging of Hg(II) by precipitation plays a more crucial role at these sites. Indeed, the annual precipitation rates on the southern slopes are generally higher than those on the northern slopes (Ceglar et al., 2016). While precipitation has been shown to have positive $\Delta^{200}\text{Hg}$ values (Gratz et al., 2010), our soils samples showed insignificant MIF of ^{200}Hg (Table S1). The absence of ^{200}Hg MIF has been explained by the dilution of Hg from frozen soils or direct deposition of Hg(0), because they are characterized by zero or negative $\Delta^{200}\text{Hg}$ values (Rolison et al., 2013; Obrist et al., 2017; Enrico et al., 2016).

Only negative $\Delta^{199}\text{Hg}$ values (−0.46 to −0.04‰) were observed in forest soils from the eastern Tibetan Plateau (Wang et al., 2017) (Figs. 2 and 4), suggesting that litterfall and direct deposition of Hg(0) are the major atmospheric Hg deposition pathways. The observation of positive $\Delta^{199}\text{Hg}$ values in our study region (Figs. 2 and 4) suggests that wet deposition could also be important in the atmospheric Hg inputs to the frozen ground of Himalaya-Tibet. This indicates that biogeochemical Hg cycling is likely different between frozen soils and forest soils in Himalaya-Tibet. Moreover, it can be seen that the southern slopes showed much larger variations of $\Delta^{199}\text{Hg}$ values than the northern slopes (Figs. 2 and 4), implying that the deposition pathways of atmospheric Hg are more diverse on the southern slopes.

4. Conclusions and implications

Our study demonstrates that Hg isotopes could provide new insights in revealing the transboundary atmospheric Hg deposition over Himalaya-Tibet. In recent decades, the emerging economies of South Asia (especially India), have become significantly

anthropogenic Hg emitters in the world (Streets et al., 2009; Pacyna et al., 2010). Their sustained economic growth has important consequences in terms of anthropogenic Hg emissions to the environment and has thus become an emerging environmental issue (Mukherjee et al., 2009; Burger Chakraborty et al., 2013). Due to its close location to Himalaya-Tibet, the impacts of atmospheric pollution from South Asia to Himalaya-Tibet must be better understood. In this study, we demonstrated that, transboundary atmospheric Hg deposition could occur in the Himalaya-Tibet. Hg concentrations and isotopic compositions of frozen soils over the Himalaya-Tibet decreased in anthropogenic signals from the southern slopes to the northern slopes, suggesting that Hg pollution was sourced from South Asia. Further we propose, the pollution of other atmospheric contaminants (e.g., black carbon, POPs) reach the Himalaya-Tibet following a similar atmospheric pathway (Cong et al., 2013; Lüthi et al., 2015; Wang et al., 2016). Due to the expected increases in the South Asian economy these contaminations may worsen.

Declaration of competing interest

We declare that we have no financial and personal relationships with other people or organizations that can inappropriately influence our work, there is no professional or other personal interest of any nature or kind in any product, service and/or company that could be construed as influencing the position presented in/or the review of the manuscript entitled “Mercury isotopes in frozen soils reveal transboundary atmospheric mercury deposition over the Himalayas and Tibetan Plateau”.

Acknowledgments

This work was supported by the National Natural Science Foundation of China (41571073; 41630754; 41421061), the Strategic Priority Research Program of Chinese Academy of Sciences (CAS), Pan-Third Pole Environment Study for a Green Silk Road (Pan-TPE) (XDA20040501), the Foundation of State Key Laboratory of Cryospheric Science, CAS (SKLCS-ZZ-2019), the Youth Innovation Promotion Association, CAS (2018094), and Academy of Finland (268170). Runsheng Yin was funded by the Chinese Academy of Sciences through the Pioneer Hundred Talent Plan. The authors appreciate all the team members of the Comprehensive Scientific Expedition to the 2013 Trans-Himalaya-Tibet for their diligent and excellent collaborative sampling work. James Hurlley from University of Wisconsin-Madison and David Krabbenhoft from United States Geological Survey are thanked for their assistance in determining Hg isotopes.

Appendix A. Supplementary data

Supplementary data to this article can be found online at <https://doi.org/10.1016/j.envpol.2019.113432>.

References

- Bergquist, B.A., Blum, J.D., 2007. Mass-dependent and-independent fractionation of Hg isotopes by photoreduction in aquatic systems. *Science* 318 (5849), 417–420.
- Blum, J.D., Sherman, L.S., Johnson, M.W., 2014. Mercury isotopes in earth and environmental sciences. *Annu. Rev. Earth Planet Sci.* 42, 249–269.
- Burger Chakraborty, L., Qureshi, A., Vadenbo, C., Hellweg, S., 2013. Anthropogenic mercury flows in India and impacts of emission controls. *Environ. Sci. Technol.* 47 (15), 8105–8113.
- Ceglar, A., Toreti, A., Balsamo, G., Kobayashi, S., 2016. Precipitation over monsoon Asia: a comparison of reanalyses and observations. *J. Clim.* 30 (2), 465–476.
- Chen, J., Hintelmann, H., Feng, X., Dimock, B., 2012. Unusual fractionation of both odd and even mercury isotopes in precipitation from Peterborough, ON, Canada. *Geochem. Cosmochim. Acta* 90, 33–46.
- Cong, Z., Kang, S., Gao, S., Zhang, Y., Li, Q., Kawamura, K., 2013. Historical trends of

- atmospheric black carbon on Tibetan Plateau as reconstructed from a 150-year lake sediment record. *Environ. Sci. Technol.* 47 (6), 2579–2586.
- Das, R., Wang, X., Khezri, B., Webster, R.D., Sikdar, P.K., Datta, S., 2016. Mercury isotopes of atmospheric particle bound mercury for source apportionment study in urban Kolkata, India. *Elementa-Sci. Anthropol.* 4 <https://doi.org/10.12952/journal.elementa.000098>.
- Demers, J.D., Blum, J.D., Zak, D.R., 2013. Mercury isotopes in a forested ecosystem: implications for air-surface exchange dynamics and the global mercury cycle. *Glob. Biogeochem. Cycles* 27 (1), 222–238.
- Enrico, M., Roux, G.L., Maruszczak, N., Heimbürger, L.-E., Claustres, A., Fu, X., Sun, R., Sonke, J.E., 2016. Atmospheric mercury transfer to peat bogs dominated by gaseous elemental mercury dry deposition. *Environ. Sci. Technol.* 50 (5), 2405–2412.
- Feng, X., Foucher, D., Hintelmann, H., Yan, H., He, T., Qiu, G., 2010. Tracing mercury contamination sources in sediments using mercury isotope compositions. *Environ. Sci. Technol.* 44, 3363–3368.
- Foucher, D., Ogrinc, Hintelmann, H., 2009. Tracing mercury contamination from the Idrija mining region (Slovenia) to the Gulf of Trieste using Hg isotope ratio measurements. *Environ. Sci. Technol.* 43 (1), 33–39.
- Gratz, L.E., Keeler, G.J., Blum, J.D., Sherman, L.S., 2010. Isotopic composition and fractionation of mercury in Great Lakes precipitation and ambient air. *Environ. Sci. Technol.* 44 (20), 7764–7770.
- Huang, J., Kang, S., Zhang, Q., Jenkins, M., Guo, J., Zhang, G., Wang, K., 2012. Spatial distribution and magnification processes of mercury in snow from high-elevation glaciers in the Tibetan Plateau. *Atmos. Environ.* 46, 140–146.
- Huang, J., Kang, S., Zhang, Q., Guo, J., Sillanpää, M., Wang, Y., Sun, S., Sun, X., Tripathee, L., 2015. Characterizations of wet mercury deposition on a remote high-elevation site in the southeastern Tibetan Plateau. *Environ. Pollut.* 206, 518–526.
- Huang, J., Kang, S., Tian, L., Guo, J., Zhang, Q., Cong, Z., Sillanpää, M., Sun, S., Tripathee, L., 2016. Influence of long-range transboundary transport on atmospheric water vapor mercury collected at the largest city of Tibet. *Sci. Total Environ.* 566–567, 1215–1222.
- Huang, J., Kang, S., Ma, M., Guo, J., Cong, Z., Dong, Z., Yin, R., Xu, J., Tripathee, L., Ram, K., Wang, F., 2019. Accumulation of atmospheric mercury in glacier cryoconite over Western China. *Environ. Sci. Technol.* 53, 6632–6639.
- Jin, H., Li, S., Cheng, G., Shaoling, W., Li, X., 2000. Permafrost and climatic change in China. *Global Planet Change* 26 (4), 387–404.
- Jiskra, M., Wiederhold, J.G., Skyllberg, U., Kronberg, R.-M., Hajdas, I., Kretzschmar, R., 2015. Mercury deposition and re-emission pathways in boreal forest soils investigated with Hg isotope signatures. *Environ. Sci. Technol.* 49 (12), 7188–7196.
- Kang, S., Xu, Y., You, Q., Flügel, W.A., Pepin, N., Yao, T., 2010. Review of climate and cryospheric change in the Tibetan Plateau. *Environ. Res. Lett.* 5 (1), 015101.
- Kang, S., Huang, J., Wang, F., Zhang, Q., Zhang, Y., Li, C., Wang, L., Chen, P., Sharma, C.M., Li, Q., 2016. Atmospheric mercury depositional chronology reconstructed from lake sediments and ice core in the Himalayas and Tibetan Plateau. *Environ. Sci. Technol.* 50 (6), 2859–2869.
- Kicińska, A., Turek, K., 2017. Establishing geochemical background of elements present in soil and its application in the evaluation of soil pollution based on data collected in the Beskid Sądecki region. *Geoinf. Pol.* 87–99.
- Kohn, M.J., 2014. Himalayan metamorphism and its tectonic implications. *Annu. Rev. Earth Planet Sci.* 42 (1), 381–419.
- Lepak, R.F., Yin, R., Krabbenhoft, D.P., Ogorek, J.M., DeWild, J.F., Holsen, T.M., Hurley, J.P., 2015. Use of stable isotope signatures to determine mercury sources in the Great Lakes. *Environ. Sci. Technol. Lett.* 2 (12), 335–341.
- Liu, Y., Dong, J., Zhang, Q., Wang, J., Han, L., Zeng, J., He, J., 2016. Longitudinal occurrence of methylmercury in terrestrial ecosystems of the Tibetan Plateau. *Environ. Pollut.* 218, 1342–1349.
- Lüthi, Z., Skerlak, B., Kim, S., Lauer, A., Mues, A., Rupakheti, M., Kang, S., 2015. Atmospheric brown clouds reach the Tibetan Plateau by crossing the Himalayas. *Atmos. Chem. Phys.* 15, 1–15.
- Mukherjee, A.B., Bhattacharya, P., Sarkar, A., Zevenhoven Bodaly, R., 2009. Mercury Emissions from Industrial Sources in India and its Effects in the Environment. Springer, New York, USA, pp. 81–112. Chap. 4.
- Obrist, D., Agnan, Y., Jiskra, M., Olson, C.L., Colegrove, D.P., Hueber, J., Moore, C.W., Sonke, J.E., Helmig, D., 2017. Tundra uptake of atmospheric elemental mercury drives Arctic mercury pollution. *Nature* 547 (7662), 201–204.
- Olson, C.L., Jiskra, M., Sonke, J.E., Obrist, D., 2019. Mercury in tundra vegetation of Alaska: spatial and temporal dynamics and stable isotope patterns. *Sci. Total Environ.* 660, 1502–1512.
- Pacyna, E.G., Pacyna, J., Sundseth, K., Munthe, J., Kindbom, K., Wilson, S., Steenhuisen, F., Maxson, P., 2010. Global emission of mercury to the atmosphere from anthropogenic sources in 2005 and projections to 2020. *Atmos. Environ.* 44 (20), 2487–2499.
- Qiu, J., 2008. The third pole. *Nature* 454 (7203), 393–396.
- Ravichandran, M., 2004. Interactions between mercury and dissolved organic matter—a review. *Chemosphere* 55, 319–331.
- Rolison, J.M., Landing, W.M., Luke, W., Cohen, M., Salters, V.J.M., 2013. Isotopic composition of species-specific atmospheric Hg in a coastal environment. *Chem. Geol.* 336, 37–49.
- Schuster, P.F., Schaefer, K.M., Aiken, G.R., Antweiler, R.C., Dewild, J.F., Gryziec, J.D., Gusmeroli, A., Hugelius, G., Jafarov, E., Krabbenhoft, D.P., Liu, L., Herman-Mercer, N., Mu, C., Roth, D.A., Schaefer, T., Striegl, R.G., Wickland, K.P., Zhang, T., 2018. Permafrost stores a globally significant amount of mercury. *Geophys. Res. Lett.* 45, 1463–1471.
- Sheng, J., Wang, X., Gong, P., Tian, L., Yao, T., 2012. Heavy metals of the Tibetan top soils. *Environ. Sci. Pollut. Res.* 19 (8), 3362–3370.
- Sheng, J., Wang, X., Gong, P., Joswiak, D.R., Tian, L., Yao, T., Jones, K.C., 2013. Monsoon-driven transport of organochlorine pesticides and polychlorinated biphenyls to the Tibetan Plateau: three year atmospheric monitoring study. *Environ. Sci. Technol.* 47 (7), 3199–3208.
- Sherman, L.S., Blum, J.D., Keeler, G.J., Demers, J.D., Dvorchak, J.T., 2012. Investigation of local mercury deposition from a coal-fired power plant using mercury isotopes. *Environ. Sci. Technol.* 46, 382–390.
- Streets, D.G., Zhang, Q., Wu, Y., 2009. Projections of global mercury emissions in 2050. *Environ. Sci. Technol.* 43 (8), 2983–2988.
- Sun, G., Sommar, J., Feng, X., Lin, C.-J., Ge, M., Wang, W., Yin, R., Fu, X., Shang, L., 2016. Mass-dependent and -independent fractionation of mercury isotope during gas-phase oxidation of elemental mercury vapor by atomic Cl and Br. *Environ. Sci. Technol.* 50 (17), 9232–9241.
- Sun, R., Sonke, J.E., Heimbürger, L.-E., Belkin, H.E., Liu, G., Shome, D., Cukrowska, E., Lioussé, C., Pokrovsky, O.S., Streets, D.G., 2014. Mercury stable isotope signatures of world coal deposits and historical coal combustion emissions. *Environ. Sci. Technol.* 48 (13), 7660–7668.
- Sun, S., Kang, S., Huang, J., Chen, S., Zhang, Q., Guo, J., Liu, W., Neupane, B., Qin, D., 2017. Distribution and variation of mercury in frozen soils of a high-altitude permafrost region on the northeastern margin of the Tibetan Plateau. *Environ. Sci. Pollut. Res.* 24 (17), 15078–15088.
- Tippling, E., Wadsworth, R., Norris, D., Hall, J., Ilyin, I., 2011. Long-term mercury dynamics in UK soils. *Environ. Pollut.* 159 (12), 3474–3483.
- UNEP, 2013. Mercury - Acting Now! United Nations Environment Programme Chemicals Branch, Geneva, Switzerland.
- Wang, X., Gong, P., Wang, C., Ren, J., Yao, T., 2016. A review of current knowledge and future prospects regarding persistent organic pollutants over the Tibetan Plateau. *Sci. Total Environ.* 573, 139–154.
- Wang, X., Luo, J., Yin, R., Yuan, W., Lin, C.J., Sommar, J., Feng, X., Wang, H., Lin, C., 2017. Using Mercury isotopes to understand mercury accumulation in the montane forest floor of the eastern Tibetan Plateau. *Environ. Sci. Technol.* 51 (2), 801–809.
- Wang, Z., Chen, J., Feng, X., Hintelmann, H., Yuan, S., Cai, H., Huang, Q., Wang, S., Wang, F., 2015. Mass-dependent and mass-independent fractionation of mercury isotopes in precipitation from Guiyang, SW China. *C. R. Geosci.* 347 (7), 358–367.
- Xu, C., Yin, R., Peng, J., Hurley, J.P., Lepak, R.F., Gao, J., Feng, X., Hu, R., Bi, X., 2018. Mercury isotope constraints on the source for sediment-hosted lead-zinc deposits in the Changdu area, southwestern China. *Miner. Depos.* 53 (3), 339–352.
- Xu, X., Zhang, Q., Wang, W., 2016. Linking mercury, carbon, and nitrogen stable isotopes in Tibetan biota: implications for using mercury stable isotopes as source tracers. *Sci. Rep.* 6, 25394.
- Xu, Z., Gong, T., Zhao, F., 2006. Analysis of climate change in Tibetan Plateau over the past 40 Years. *J. Subtrop. Res. Environ.* 1 (1), 24–32 (in Chinese with English abstract).
- Yao, T., Thompson, L.G., Mosbrugger, V., Zhang, F., Ma, Y., Luo, T., Xu, B., Yang, X., Joswiak, D.R., Wang, W., Joswiak, M.E., Devkota, L.P., Tayal, S., Jilani, R., Fayziev, R., 2012. Third Pole environment (TPE). *Environ. Dev.* 3, 52–64.
- Yin, R., Feng, X., Meng, B., 2013. Stable mercury isotope variation in rice plants (*Oryza sativa* L.) from the Wanshan mercury mining district, SW China. *Environ. Sci. Technol.* 47 (5), 2238–2245.
- Yin, R., Krabbenhoft, D.P., Bergquist, B.A., Zheng, W., Lepak, R.F., Hurley, J.P., 2016a. Effects of mercury and thallium concentrations on high precision determination of mercury isotopic composition by Neptune Plus multiple collector inductively coupled plasma mass spectrometry. *J. Anal. Atomic Spectrom.* 31 (10), 2060–2068.
- Yin, R., Feng, X., Hurley, J.P., Krabbenhoft, D.P., Lepak, R.F., Kang, S., Yang, H., Li, X., 2016b. Historical records of mercury stable isotopes in sediments of Tibetan lakes. *Sci. Rep.* 6, 23332. <https://doi.org/10.1038/srep23332>.
- Yang, H., Battarbee, R.W., Turner, S.D., Rose, N.L., Derwent, R.G., Wu, G., Yang, R., 2010. Historical reconstruction of mercury pollution across the Tibetan Plateau using lake sediments. *Environ. Sci. Technol.* 44 (8), 2918–2924.
- Yang, R., Xie, T., Li, A., Yang, H., Turner, S., Wu, G., Jing, C., 2016. Sedimentary records of polycyclic aromatic hydrocarbons (PAHs) in remote lakes across the Tibetan Plateau. *Environ. Pollut.* 214, 1–7.
- Yuan, S., Zhang, Y., Chen, J., Kang, S., Zhang, J., Feng, X., Cai, H., Wang, Z., Wang, Z., Huang, Q., 2015. Large variation of mercury isotope composition during a single precipitation event at Lhasa City, Tibetan Plateau, China. *Procedia Earth Planet. Sci.* 13, 282–286.
- Zhang, H., Yin, R., Feng, X., Sommar, J., Anderson, C.W., Sapkota, A., Fu, X., Larssen, T., 2013. Atmospheric mercury inputs in montane soils increase with elevation: evidence from mercury isotope signatures. *Sci. Rep.* 3, 3322.
- Zheng, W., Hintelmann, H., 2009. Mercury isotope fractionation during photoreduction in natural water is controlled by its Hg/DOC ratio. *Geochem. Cosmochim. Acta* 73 (22), 6704–6715.
- Zheng, W., Obrist, D., Weis, D., Bergquist, B.A., 2016. Mercury isotope compositions across North American forests. *Glob. Biogeochem. Cycles* 30 (10), 1475–1492.